

Evolution of magnetic interactions in a pressure-induced Jahn-Teller driven magnetic dimensionality switch

S. Ghannadzadeh,^{1,*} J. S. Möller,^{1,†} P. A. Goddard,¹ T. Lancaster,² F. Xiao,² S. J. Blundell,¹ A. Maisuradze,³ R. Khasanov,³ J. L. Manson,⁴ S. W. Tozer,⁵ D. Graf,⁵ and J. A. Schlueter⁶

¹Clarendon Laboratory, Department of Physics, University of Oxford, Parks Road, Oxford, OX1 3PU, United Kingdom

²Department of Physics, Durham University, South Road, Durham, DH1 3LE, United Kingdom

³Laboratory for Muon Spin Spectroscopy, Paul Scherrer Institut, CH-5232 Villigen PSI, Switzerland

⁴Department of Chemistry and Biochemistry, Eastern Washington University, Cheney, Washington 99004, USA

⁵National High Magnetic Field Laboratory, Florida State University, Tallahassee, Florida 32310, USA

⁶Materials Science Division, Argonne National Laboratory, Argonne, Illinois 60439, USA

(Received 25 February 2013; published 12 June 2013)

We present the results of high-field magnetization and muon-spin relaxation measurements on the coordination polymer $\text{CuF}_2(\text{H}_2\text{O})_2(\text{pyrazine})$ in pressures up to 22.5 kbar. We observe a transition from a quasi-two-dimensional to a quasi-one-dimensional antiferromagnetic phase at 9.1 kbar, driven by a rotation of the Jahn-Teller axis. Long-range antiferromagnetic ordering is seen in both regimes, as well as a phase separation in the critical pressure region. The magnetic dimensionality switching as pressure is increased is accompanied by a halving of the primary magnetic exchange energy J and a fivefold decrease in the ordering temperature T_N . J decreases gradually with pressure in the two-dimensional phase, and then increases in the one-dimensional regime. We relate both effects to the changes in the crystal structure with applied pressure.

DOI: [10.1103/PhysRevB.87.241102](https://doi.org/10.1103/PhysRevB.87.241102)

PACS number(s): 75.30.Et, 62.50.-p, 75.30.Kz, 75.50.Ee

Pressure plays a central role in the exploration of physical phenomena, for example, in metal-insulator transitions^{1,2} and superconductivity.^{3,4} This is because it allows a controlled adjustment of structural parameters, such that their influence on the electronic and magnetic properties can be determined. Pressure can also affect transition-metal coordination polymers, which are important candidates for the future development of purpose-engineered magnetic materials.⁵ A portion of such polymeric magnets are based on heteroligand Jahn-Teller (JT)⁶ active metal centers, where the transition metal ion sits in a position of octahedral symmetry, surrounded by an asymmetric ligand environment. In such systems each *trans*-coordinated ligand provides an additional degree of freedom on the JT axis, meaning that small perturbations of the metal-ligand environment can be enough to rotate the JT axis and radically modify the material properties. Pressure presents an ideal method of systematically achieving such perturbations, due to the relative softness and high compressibility of the organic framework. It has recently been shown that it is possible to select the magnetic dimensionality of polymeric magnets at the synthesis stage.⁷ In this Rapid Communication we will show that pressure can be used to operate a Jahn-Teller driven magnetic dimensionality switch, between a two-dimensional and a one-dimensional antiferromagnetic phase, in the extended Cu-based coordination network $\text{CuF}_2(\text{H}_2\text{O})_2(\text{pyz})$ ($\text{pyz} = \text{pyrazine}, \text{C}_4\text{H}_4\text{N}_2$). In this compound, hydrogen-bonding interactions, a JT-active metal center, and three different *trans*-coordinated ligands promote significant pressure-induced structural transitions. Together, these features enable pressure-induced perturbation of the magnetic exchange, allowing the modification of the system's magnetic dimensionality and providing the ability to tune the primary exchange energy J .

$\text{CuF}_2(\text{H}_2\text{O})_2(\text{pyz})$ has a strongly anisotropic structure, consisting of Cu-pyz-Cu chains along the crystallographic a

axis, with the Cu^{2+} metal centers also joined together via a two-dimensional hydrogen-bonding lattice in the bc plane, as shown in Fig. 1. The spin-1/2 Cu atom sits at the center of a distorted octahedron, surrounded by *trans* pairs of Cu-O, Cu-F, and Cu-N ligands. At ambient pressure the elongated JT axis is oriented along the N-Cu-N bonds, implying that the $d_{x^2-y^2}$ orbitals and the directions of largest electronic overlap are directed perpendicular to this axis, and are within the bc plane. This situation is confirmed by pulsed-field magnetization, electron-spin resonance (ESR), muon-spin relaxation ($\mu^+\text{SR}$), and neutron scattering measurements,^{8,9} showing that the compound displays highly two-dimensional antiferromagnetic behavior ($J = 11.5$ K, secondary exchange energy $J_{\perp} \sim 10^{-4} J$, long-range ordering temperature $T_N = 2.6$ K), with the primary magnetic exchange mediated via the Cu-OH \cdots F-Cu spin exchange paths within the bc planes. The crucial role of the H \cdots F bonds in mediating exchange has also been investigated through selective isotopic H substitution.¹⁰

Recent synchrotron x-ray powder diffraction measurements by Halder *et al.*¹¹ have revealed that $\text{CuF}_2(\text{H}_2\text{O})_2(\text{pyz})$ undergoes two structural phase transitions as a function of pressure, accompanied by a rotation of the JT axis and orbital orientations. With the application of pressure, the elongated JT axis was found to change from the Cu-N to the Cu-O bond direction at $P_c \approx 9$ kbar. This shift was also detected in single-crystal diffraction experiments, albeit at the higher pressure of 18 kbar.¹² A further pressure-induced change to the Cu-F direction was seen by Halder *et al.*¹¹ at 31 kbar.

In this Rapid Communication we report a profound change in the magnetic properties occurring at 9.1 kbar in both single-crystal and powder samples. Our interpretation of this result is consistent with the rotation of the JT axis observed by Halder *et al.*¹¹ At this pressure the magnetic structure switches from quasi-two-dimensional (Q2D) to quasi-one-dimensional (Q1D) due to the reorientation of the $d_{x^2-y^2}$

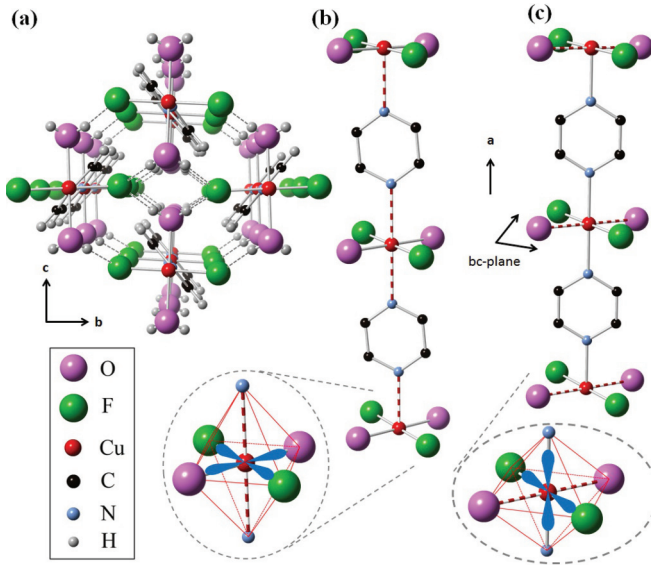


FIG. 1. (Color online) Crystal structure of $\text{CuF}_2(\text{H}_2\text{O})_2(\text{pyz})$ (Refs. 8 and 11), showing (a) the 2D hydrogen bonding network at ambient pressure. Hydrogen positions are approximate. Also shown is an isolated Cu-pyz-Cu chain at (b) ambient pressure and (c) 13.9 kbar, on the same scale. The JT axis is shown by the red striped bonds. The zoomed-in regions show the JT octahedron, together with a representation of the magnetic orbitals, which provide the dominant exchange pathways.

orbitals, from lying within the hydrogen-bonded bc plane to the ac plane—thus significantly decreasing the electronic overlap along the Cu-OH \cdots F-Cu bonds, while simultaneously increasing the magnetic orbital overlap along the a axis.¹¹ This results in the primary exchange being mediated by pyrazine molecules via the Cu-pyz-Cu chain, therefore allowing Q1D antiferromagnetism to develop. To establish this pressure-induced dimensional switching, as well as to track the evolution of magnetic energies, the behavior of $\text{CuF}_2(\text{H}_2\text{O})_2(\text{pyz})$ as a function of pressure was explored using high-field magnetization and μ^+ SR.

Single-crystal magnetization measurements in fields up to 35 T were performed at the National High Magnetic Field Laboratory (NHMFL, USA) using a radio-frequency technique that has recently been shown to be an effective method of obtaining magnetic susceptibility, and hence, magnetization.^{13,14} Measurements were performed at 1.4 K, with the applied magnetic field parallel to the Cu-pyz-Cu chain direction. A piston cylinder cell was used to achieve the pressure. The pressure was measured *in situ* by using the fluorescence of ruby, which showed good hydrostatic conditions.¹⁴ Two measurements were performed in the low-pressure regime ($P < P_c$), another at the critical pressure P_c , and a further three in the high-pressure region ($P > P_c$).

The magnetization, measured across a range of pressures up to 20 kbar, is given in Fig. 2(a). At ambient pressure the magnetization rises monotonically with a curvature typical of Q2D antiferromagnetic systems,⁷ saturating at 28.1 T, in agreement with previous measurements.⁸ As pressure is applied, we observe a steady reduction in the critical field B_c , down to 23.4 T at 9.1 kbar [see Fig. 2(c)]. Further application of pressure leads to a dramatic drop in B_c to 8.3 T, after which any additional pressure serves to gradually increase the saturation field, in contrast to the behavior seen at lower pressures.

The magnetism in $\text{CuF}_2(\text{H}_2\text{O})_2(\text{pyz})$ can be described by the Heisenberg model

$$\mathcal{H} = J \sum_{\langle i,j \rangle_{\parallel}} \mathbf{S}_i \cdot \mathbf{S}_j + J_{\perp} \sum_{\langle i,j \rangle_{\perp}} \mathbf{S}_i \cdot \mathbf{S}_j - g\mu_B B \sum_i S_i^z,$$

where in a Q2D (Q1D) phase, J and J_{\perp} are the magnetic exchange strengths within and normal to the planes (chains), respectively. The first two summations are over the unique ligands through which the exchange coupling takes place, and the last term is the Zeeman splitting term. For a Heisenberg spin-1/2 antiferromagnet (AFM) the form of the magnetization up to saturation strongly reflects the magnetic dimensionality, and quantum Monte Carlo simulations have shown that the magnetization becomes strongly concave as the dimensionality is reduced.¹⁵ Indeed, looking at Fig. 2(b), the magnetization becomes noticeably concave above 9.1 kbar, an indication of the reduction in the magnetic dimensionality. Moreover,

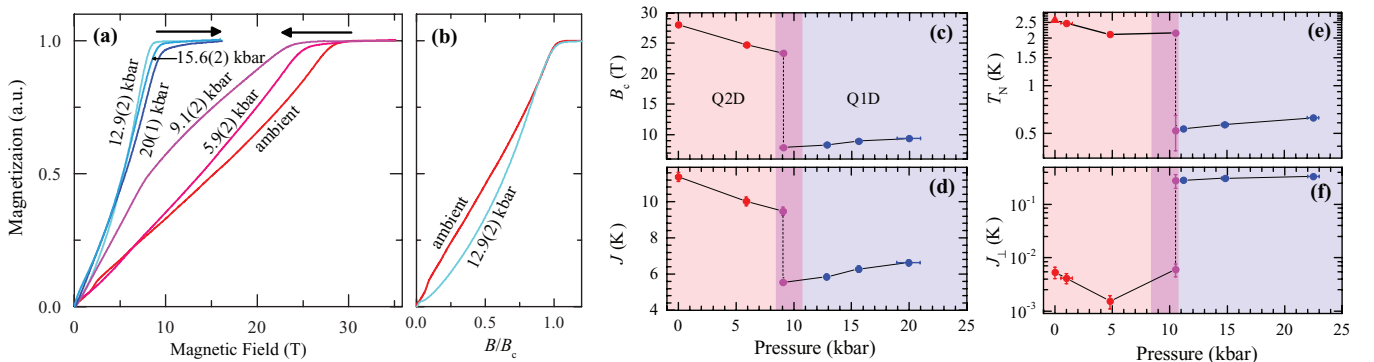


FIG. 2. (Color online) (a) Magnetization of $\text{CuF}_2(\text{H}_2\text{O})_2(\text{pyz})$ single crystals with $B \parallel a$ axis, at 1.4 K (2 K at 15.6 kbar). The arrows represent the change in the saturation field with increasing pressure. (b) M vs B/B_c at ambient pressure and 12.9 kbar, showing the change in curvature. Also shown is (c) the saturation field B_c , (d) the deduced primary exchange coupling energy J , (e) the ordering temperature T_N deduced from the μ^+ SR data (see Fig. 3), and (f) the secondary exchange J_{\perp} . To extract J , we have used values of g obtained from ESR measurements (Ref. 12). T_N at ambient pressure (triangle symbol) is from Ref. 8.

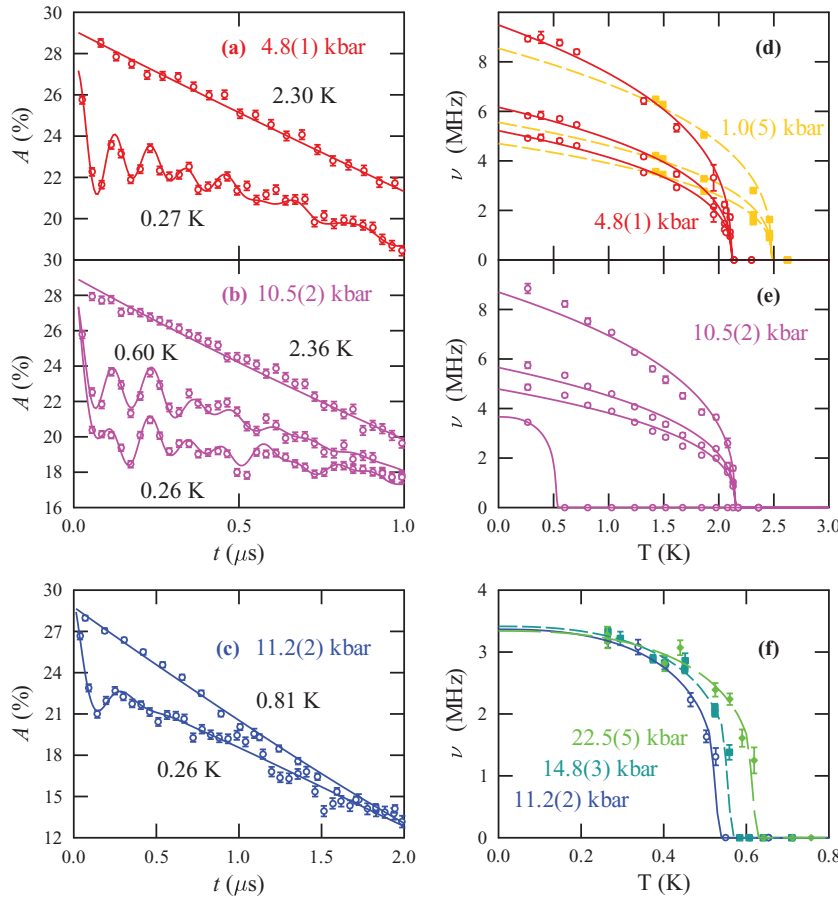


FIG. 3. (Color online) Time evolution of the μ^+ decay asymmetry $A(t)$ in (a), (b) the low-pressure regime, and (c) the high-pressure phase. Also shown are (d)–(f) the fitted oscillation frequencies $\nu(T)$. Three frequencies were dominant in the low-pressure regime, while the higher-pressure phase was well described by a single frequency. The lines in (d)–(f) represent fits to $\nu(T) = \nu_0[1 - (T/T_N)^\alpha]^\beta$, where α and β were fixed to 1 (2.5) and 0.36 (0.3) in the Q2D (Q1D) phases, respectively.

looking at the 9.1 kbar data, we discover a noticeable change in the magnetization gradient at a field (7.9 T) close to the critical field of the higher-pressure phase. The curvature of the magnetization below this field is similar to that of the higher-pressure regime, while the curvature above it is closer to that seen at low pressures [see Fig. 2(a)]. This implies a degree of phase separation, with coexisting volumes of the sample in the high- and low-pressure phases.

The fact that both the phase separation and the change in curvature occur at the same pressure as the JT-axis shift¹¹ leads us to conclude that the dramatic drop in B_c above 9.1 kbar is due to the proposed transition from the Q2D to a Q1D antiferromagnetic phase. In a strongly anisotropic system ($J_\perp \ll J$), we can express the saturation field as $B_c \approx nJ/g\mu_B$, where n is the number of nearest-neighbor exchange ligands of interaction strength J ($n = 4$ for Q2D, 2 for Q1D), and g is the g factor.¹⁵ The sudden change in B_c can thus be understood as a combination of the change in n from 4 to 2 (i.e., a Q2D to Q1D transition), and a simultaneous change in J .

The extracted values of J are given in Fig. 2(d). We find $J \approx 11.4$ K at ambient pressure, confirming previous pulsed-field measurements.⁸ Under application of moderate pressures, J begins to decrease gradually at a rate of 0.21 ± 0.01 K/kbar, eventually reaching 9.5 K at 9.1 kbar. A further increase in pressure leads to a substantial reduction in J , down to 5.5 K, caused by the switching of the main exchange pathways to bonds with weaker effective nearest-neighbor interactions as the system undergoes a change in magnetic dimensionality.

Within the high-pressure region, any further application of pressure results in a steady increase in J at the rate of 0.1 ± 0.01 K/kbar.

Further support for the dimensionality switch comes from μ^+ SR measurements which probe the magnetic ordering of a system and allow one to extract T_N .¹⁶ Powder sample μ^+ SR measurements were carried out at the Swiss Muon Source, with detailed temperature scans taken at six different pressures using a piston cylinder cell, which showed good hydrostaticity.¹⁴ Example μ^+ SR spectra are given in Figs. 3(a)–3(c). The μ^+ SR data were fitted to

$$A(t) = \sum_i A_i e^{-\lambda_i t} \cos(2\pi \nu_i t + \phi_i) + \sum_i A_i e^{-\lambda_i t} + A_b(t),$$

where ν_i are the dominant oscillation frequencies due to long-range magnetic order of the sample, ϕ_i is a constant phase, the exponential terms account for residual magnetic dynamics in the sample, and $A_b(t)$ accounts for the background from the pressure cell.¹⁴

The evolution of the fitted oscillation frequencies is given in Figs. 3(d)–3(f). Within the low-pressure regime, we observe oscillations at three frequencies below a critical temperature, which at approximately 1 kbar is 2.48(1) K. This is in agreement with previous ambient pressure measurements which found oscillations at three frequencies below 2.59(1) K.⁸ In this regime, T_N is found to decrease with application of pressure [see Fig. 2(e)].

At 11.2 kbar and above there is no discontinuous change in the μ^+ SR spectra above 1 K. However, oscillations at

a single frequency appear below 630 mK [Figs. 3(c) and 3(f)], providing evidence for long-range magnetic order in the high-pressure regime. T_N is found to increase with increasing pressure, in accordance with the behavior of the dominant exchange J , and the change in T_N is found to be reversible upon reduction of pressure from 22.5 to 11.2 kbar. Compared to a Q2D system, a Q1D system should be expected to have a much reduced long-range ordering temperature owing to the increased influence of fluctuations in one dimension. Therefore, the large decrease in T_N that we observe in the critical pressure region [Fig. 2(e)] is consistent with a transition to Q1D magnetic behavior at high pressures. Also note the different temperature dependence of the oscillation frequencies in the Q1D and Q2D phases.

The combination of a substantial change in the μ^+ SR frequencies and ordering temperature T_N , as well as a dramatic reduction in the critical field B_c , provides unambiguous evidence and direct confirmation of the proposed phase transition from Q2D to Q1D antiferromagnetism. We emphasize that the critical pressure region of 9.1 kbar is in agreement with the critical pressure of the JT-axis change seen in powder-sample structural measurements.¹¹ This dimensionality crossover is further supported by an ESR study, which observed reorientation of the magnetic d orbitals at the pressure-induced JT-axis shift.¹²

Given the values of J and T_N , we can estimate the secondary exchange energy J_\perp by using the empirical relations $|J_\perp| = |J| \exp(2.43 - 0.88\lambda)$ for the Q2D phase, and $|J_\perp| = 1.073T_N(\ln\lambda + 0.5\ln\ln\lambda)^{-1/2}$ for the Q1D phase, where $\lambda = 2.6J/T_N$.¹⁷ The calculated values of J_\perp are shown in Fig. 2(f). Within the low-pressure Q2D phase we find J_\perp to be of the order of 1 mK. In the Q1D regime, J_\perp is mediated by the portion of the $d_{x^2-y^2}$ orbitals that still lie within the bc plane, and this leads to a jump in J_\perp by two orders of magnitude to approximately 0.3 K as we move over to the Q1D phase.

Quantum fluctuations significantly reduce the size of the ordered moment in low-dimensional AFMs. Using a mean-field approximation, we can estimate the zero-field moment of a Q1D AFM from $m_0 = 2.034\sqrt{J_\perp/J} \mu_B$.¹⁸ The value of J_\perp/J remains approximately constant within the Q1D phase, yielding a value of $m_0 = 0.46 \pm 0.01\mu_B$. This compares with $0.5\mu_B$ and $0.072\mu_B$ in the Q1D AFMs KCuF_3 and Sr_2CuO_3 .¹⁸ We expect nearly the full Cu moment of $1\mu_B$ in the Q2D phase.¹⁴

The trends in J [Fig. 2(d)] can be explained in terms of the effect of pressure on the crystal structure and the magnetic exchange ligands. The decrease seen in J within the Q2D phase is due to the increase in the β angle between the a and c axes,¹¹ which leads to a misalignment of Cu-pyz-Cu chains and causes them to begin to slide past each other.¹⁹ This serves to severely disrupt the $\text{H}\cdots\text{F}$ bonded network, decreasing the efficiency of magnetic coupling along the $\text{Cu-OH}\cdots\text{F-Cu}$ exchange pathways and thus reducing J .

The steady increase in J with applied pressure within the Q1D regime is because unlike the soft $\text{H}\cdots\text{F}$ bonded layers, the Cu-N bonds, and the pyrazine rings are relatively resilient, and so no major distortions are seen within the Cu-pyz-Cu chain in the Q1D regime.^{11,19} This resiliency, together with the decrease in the chain length with applied pressure,¹¹ enhances the magnetic d -orbital density overlap along the chain and results in the increase in J .

The μ^+ SR data provide evidence for phase separation at 10.5 kbar, where a fourth frequency appears at low temperatures and the other three frequencies remain present up to 2.15 K [see Fig. 3(e)]. The magnitude of the fourth frequency is consistent with those found for the Q1D ordering at 11.2 kbar and above, and the other three frequencies are consistent with those found for the Q2D ordering below 10 kbar. While we cannot completely rule out the effects of nonhydrostaticity,²⁰ these observations in both powder μ^+ SR and single-crystal magnetization measurements, as well as in the separate ESR study,¹² seem to point towards the presence of an intrinsic phase separation in the critical pressure region, reminiscent of the phase separation frequently observed close to some pressure-induced quantum phase transitions.²¹

We observe that in $\text{CuF}_2(\text{H}_2\text{O})_2(\text{pyz})$, the presence of three different ligands in the Cu-centered octahedra effectively introduced several degrees of freedom in the JT-axis orientation. This has allowed a sequential change in the direction of the JT axis through structural perturbations, due to the different ligand strengths. It is interesting to compare this material to $\text{Cu}(\text{NO}_3)_2(\text{pyz})$, which is similarly based on a JT-active Cu atom sitting in a distorted octahedron, but only surrounded by two unique ligands.¹⁴ This system is known to be a Q1D AFM at ambient pressure, with the magnetic orbitals lying within the Cu-pyz-Cu chain direction and the JT axis along the Cu-O bonds.²² Unlike $\text{CuF}_2(\text{H}_2\text{O})_2(\text{pyz})$, no JT switching or orbital reorientation is seen upon application of pressure (up to 11.6 kbar) in this compound, due to the angle of the O-Cu-O bonds in the octahedra being significantly different from 90° .¹⁴ Such a mismatch with the symmetry of the $d_{x^2-y^2}$ orbitals would considerably increase the energy cost of an orbital reorientation. Furthermore, in $\text{CuF}_2(\text{H}_2\text{O})_2(\text{pyz})$, the change in JT axis from Cu-N to Cu-O, to Cu-F, leads to a sequential decrease in the unit cell volume with increasing pressure. In contrast, a rotation of JT distortion axis from Cu-O to Cu-N in $\text{Cu}(\text{NO}_3)_2(\text{pyz})$ could potentially lead to an increase in the unit cell volume, which is energetically unfavorable.

In summary, we have shown that pressure can be used to induce a Jahn-Teller driven magnetic dimensionality switch in $\text{CuF}_2(\text{H}_2\text{O})_2(\text{pyz})$, due to a change in the primary magnetic exchange pathways. Thus pressure can be used to take control of the magnetic properties of metal-polymeric systems, giving us the ability to tune the interaction strengths and select the magnetic dimensionality via external perturbation. This work emphasizes the powerful role that pressure can play in exploring new materials and phases, especially in heteroligand complexes with active Jahn-Teller centers.

This work is supported by EPSRC (U.K.). A portion of this work was performed at the National High Magnetic Field Laboratory, which is supported by NSF Cooperative Agreement No. DMR-0654118, the State of Florida, and the DOE. The muon experiment was performed on the GPD instrument at the Swiss Muon Source, Paul Scherrer Institut, Switzerland. Work supported by Argonne, a DOE Office of Science laboratory, operated under Contract No. DE-AC02-06CH11357. D.G. and S.W.T. are supported by DOE/NNSA Grant No. DE-FG52-10NA29659. The work at EWU was supported by NSF Grant No. DMR-1005825.

*s.ghannadzadeh1@physics.ox.ac.uk

†j.moeller1@physics.ox.ac.uk for μ^+ SR details.

- ¹H. Okabe, N. Takeshita, M. Isobe, E. Takayama-Muromachi, T. Muranaka, and J. Akimitsu, *Phys. Rev. B* **84**, 115127 (2011).
- ²A. Irizawa, S. Suga, G. Isoyama, K. Shimai, K. Sato, K. Iizuka, T. Nanba, A. Higashiya, S. Niitaka, and H. Takagi, *Phys. Rev. B* **84**, 235116 (2011).
- ³D. Graf, R. Stillwell, T. P. Murphy, J. H. Park, E. C. Palm, P. Schlottmann, R. D. McDonald, J. G. Analytis, I. R. Fisher, and S. W. Tozer, *Phys. Rev. B* **85**, 134503 (2012).
- ⁴T. Park *et al.*, *Nature (London)* **440**, 65 (2006).
- ⁵S. J. Blundell, *Contemp. Phys.* **48**, 275 (2007).
- ⁶H. A. Jahn and E. Teller, *Proc. R. Soc. London* **161**, 220 (1937).
- L. R. Falvello, *J. Chem. Soc. Dalton Trans.* **23**, 4463 (1997).
- ⁷P. A. Goddard *et al.*, *Phys. Rev. Lett.* **108**, 077208 (2012).
- ⁸J. L. Manson *et al.*, *Chem. Mater.* **20**, 7408 (2008).
- ⁹C. H. Wang *et al.*, *Phys. Rev. B* **86**, 064439 (2012).
- ¹⁰P. A. Goddard *et al.*, *Phys. Rev. B* **78**, 052408 (2008).
- ¹¹G. J. Halder *et al.*, *Angew. Chem. Int. Ed.* **50**, 419 (2011).
- ¹²A. Prescimone *et al.*, *Angew. Chem. Int. Ed.* **51**, 7490 (2012).
- ¹³S. Ghannadzadeh *et al.*, *Rev. Sci. Instrum.* **82**, 113902 (2011).
- ¹⁴See Supplemental Material at <http://link.aps.org/supplemental/10.1103/PhysRevB.87.241102> for experimental details, the structure of $\text{Cu}(\text{NO}_3)_2(\text{pyz})$, and a discussion of low-field magnetic susceptibility measurements.
- ¹⁵P. A. Goddard *et al.*, *New J. Phys.* **10**, 083025 (2008).
- ¹⁶S. J. Blundell, *Contemp. Phys.* **40**, 175 (1999).
- ¹⁷C. Yasuda, S. Todo, K. Hukushima, F. Alet, M. Keller, M. Troyer, and H. Takayama, *Phys. Rev. Lett.* **94**, 217201 (2005).
- ¹⁸H. J. Schulz, *Phys. Rev. Lett.* **77**, 2790 (1996).
- ¹⁹J. L. Musfeldt *et al.*, *Inorg. Chem.* **50**, 6347 (2011).
- ²⁰The hydrostaticity is estimated to be ± 0.2 kbar for the 10.5 kbar μ^+ SR experiment. We also estimate an upper limit of ± 0.7 kbar for the 9.1 kbar magnetization measurement (Ref. 14).
- ²¹C. Pfleiderer, *J. Phys.: Condens. Matter* **17**, S987 (2005).
- ²²T. Lancaster, S. J. Blundell, M. L. Brooks, P. J. Baker, F. L. Pratt, J. L. Manson, C. P. Landee, and C. Baines, *Phys. Rev. B* **73**, 020410 (2006).